

Published in final edited form as:

*Kidney Int.* 2010 August ; 78(4): 363–373. doi:10.1038/ki.2010.137.

## Inhibition of integrin-linked kinase blocks podocyte epithelial–mesenchymal transition and ameliorates proteinuria

Young Sun Kang<sup>1,2</sup>, Yingjian Li<sup>1,2</sup>, Chunsun Dai<sup>1</sup>, Lawrence P. Kiss<sup>1</sup>, Chuanyue Wu<sup>1</sup>, and Youhua Liu<sup>1</sup>

<sup>1</sup>Department of Pathology, University of Pittsburgh School of Medicine, Pittsburgh, Pennsylvania, USA

### Abstract

Proteinuria is a primary clinical symptom of a large number of glomerular diseases that progress to end-stage renal failure. Podocyte dysfunctions play a fundamental role in defective glomerular filtration in many common forms of proteinuric kidney disorders. Since binding of these cells to the basement membrane is mediated by integrins, we determined the role of integrin-linked kinase (ILK) in podocyte dysfunction and proteinuria. ILK expression was induced in mouse podocytes by various injurious stimuli known to cause proteinuria including TGF- $\beta$ 1, adriamycin, puromycin, and high ambient glucose. Podocyte ILK was also found to be upregulated in human proteinuric glomerular diseases. Ectopic expression of ILK in podocytes decreased levels of the epithelial markers nephrin and ZO-1, induced mesenchymal markers such as desmin, fibronectin, matrix metalloproteinase-9 (MMP-9), and  $\alpha$ -smooth muscle actin ( $\alpha$ -SMA), promoted cell migration, and increased the paracellular albumin flux across podocyte monolayers. ILK also induced Snail, a key transcription factor mediating epithelial–mesenchymal transition (EMT). Blockade of ILK activity with a highly selective small molecule inhibitor reduced Snail induction and preserved podocyte phenotypes following TGF- $\beta$ 1 or adriamycin stimulation. *In vivo*, this ILK inhibitor ameliorated albuminuria, repressed glomerular induction of MMP-9 and  $\alpha$ -SMA, and preserved nephrin expression in murine adriamycin nephropathy. Our results show that upregulation of ILK is a convergent pathway leading to podocyte EMT, migration, and dysfunction. ILK may be an attractive target for therapeutic intervention of proteinuric kidney diseases.

### Keywords

adriamycin; integrin-linked kinase; podocyte; proteinuria

---

Proteinuria, the clinical manifestation of a defective glomerular filtration, is an early hallmark of a large number of glomerular diseases that progress to end-stage kidney failure.<sup>1,2</sup> Glomerular filtration barrier consists of fenestrated endothelium, glomerular basement membrane, and terminally differentiated podocytes, which possess sophisticated foot processes that extend toward the capillaries to which they affix.<sup>3</sup> Podocyte foot processes interdigitate with the counterparts of their neighboring cells to form filtration slits,

---

© 2010 International Society of Nephrology

**Correspondence:** Youhua Liu, Department of Pathology, University of Pittsburgh School of Medicine, S405 Biomedical Science Tower, 200 Lothrop Street, Pittsburgh, Pennsylvania 15261, USA. liuy@upmc.edu.

<sup>2</sup>These authors contributed equally to this work.

### DISCLOSURE

All the authors declared no competing interests.

known as the slit diaphragm. This membrane-like structure constitutes the final barrier to protein loss during the convective fluid flow from vascular to urinary space of the capillary wall.<sup>4,5</sup> In this context, the slit diaphragm of podocyte foot processes is the major determinant of the size permselectivity of glomerular filtration barrier. Accordingly, any injury to podocytes that disrupts the structural and functional integrity of the slit diaphragm would eventually lead to a defective glomerular filtration, thereby causing proteinuria in various pathologic circumstances.

Podocytes are susceptible to injury as seen in many forms of glomerular diseases, including diabetic nephropathy, focal segmental glomerulosclerosis, membranous glomerulopathy, and lupus nephritis.<sup>6–8</sup> How injurious stimuli cause podocyte damage leading to proteinuria, however, remains elusive and controversial. A prevalent view in the field emphasizes on the importance of podocyte depletion, resulted from the detachment from the glomerular basement membrane and/or apoptosis, as a causative factor for the onset of proteinuria.<sup>2,9–12</sup> Emerging evidence also suggests that podocytes could undergo a phenotypic conversion after injury, characterized by losing its epithelial features such as nephrin, P-cadherin, and ZO-1, while acquiring mesenchymal markers such as desmin, fibroblast-specific protein-1, matrix metalloproteinase-9 (MMP-9), type I collagen, and fibronectin.<sup>13–15</sup> This epithelial–mesenchymal transition (EMT) will render podocytes motile and ultimately lead to the disruption of the delicate three-dimensional architecture of podocytes, thereby impairing their filtration barrier function.<sup>16</sup> However, the underlying mechanism as well as the intracellular mediator that governs podocyte EMT under pathologic conditions remains largely unknown.

Integrin-linked kinase (ILK) is an ankyrin repeat-containing serine/threonine protein kinase that interacts with the cytoplasmic domains of  $\beta 1$  and  $\beta 3$  integrins and mediates the integrin signaling.<sup>17,18</sup> ILK has been shown to have an essential role in podocyte biology, as conditional knockout of its gene in a podocyte-specific manner leads to massive proteinuria, glomerulosclerosis, kidney failure, and premature death in mice.<sup>19,20</sup> Aberrant regulation of ILK is also implicated in the pathogenesis of various proteinuric kidney diseases including diabetic nephropathy, congenital nephritic syndrome, experimental models of glomerular disease.<sup>21–23</sup> In addition, ILK is shown to be a key intracellular mediator that controls EMT in tubular epithelial cells.<sup>24</sup> These observations point to a possible connection among aberrant ILK regulation, podocyte EMT, dysfunction, and proteinuria.

In this study, we have investigated the regulation and function of ILK in cultured podocytes and in mouse model of podocyte injury induced by adriamycin (ADR). We found that ILK expression in podocytes is increased in response to various injurious stimuli, and ectopic expression of ILK induces Snail and mesenchymal conversion of podocytes. Furthermore, administration of a small molecule ILK inhibitor *in vivo* ameliorates albuminuria and protects podocytes from injury. Our results indicate that increased ILK has a role in mediating podocyte dysfunction, and thus targeting this signaling could be an attractive strategy for therapeutic intervention of proteinuric kidney diseases.

## RESULTS

### Upregulation of ILK in podocytes after various injuries

To investigate the potential role of ILK in podocyte dysfunction, we evaluated the effects of various extracellular cues on ILK expression in cultured mouse podocytes. As shown in Figure 1a and b, transforming growth factor (TGF)- $\beta 1$  induced ILK expression in a time-dependent manner, and substantial increase in ILK protein level was observed at 24 h after TGF- $\beta 1$  stimulation. Dose–response studies revealed that TGF- $\beta 1$  at 2 ng/ml induced maximal expression of ILK, and further increase in TGF- $\beta 1$  beyond this concentration did

not result in additional induction (Figure 1c). Immunofluorescence staining also showed a dramatic induction of ILK after TGF- $\beta$ 1 treatment (Figure 1d). ILK was localized primarily in the focal adhesion sites that have close contacts between the substrate and the plasma membrane on the basal surface of podocytes (Figure 1d, arrowheads). Of interest,  $\beta$ 1 integrin, the upstream regulator of ILK, was also upregulated in the injured podocytes after TGF- $\beta$ 1 treatment (Figure 1e).

We also examined ILK expression in podocytes after treatment with various injurious stimuli. As shown in Figure 2, ADR, a well-known agent that specifically damages podocytes and causes proteinuria *in vivo*,<sup>25,26</sup> induced ILK expressions in a time- and dose-dependent manner. Similarly, puromycin aminonucleoside (PAN) also induced ILK expression in podocytes (Figure 2c and d). The induction of ILK in podocytes occurred rapidly, beginning between 1 and 6 h after ADR or PAN treatment (Figure 2a and c). We found that high ambient glucose condition also induced ILK expression in a delayed manner, compared with normal glucose condition or mannitol controls (Figure 2e). Together, these results suggest that upregulation of ILK is a common response of podocytes following different stresses/injuries.

### Specific induction of ILK in podocytes in primary glomerular diseases

To explore the relevance of ILK regulation to podocyte dysfunction *in vivo*, we examined ILK protein expression in the glomeruli of human kidneys with primary glomerular diseases. Immunohistochemical staining showed little ILK protein in normal glomeruli of human kidneys (Figure 3a). However, ILK protein was upregulated in the glomeruli of kidney biopsies from patients with focal segmental glomerulosclerosis (Figure 3b and c). On the basis of anatomical location and morphology, these ILK-positive cells appeared to be podocytes. Similarly, ILK was also upregulated in the glomerular podocytes in kidney biopsies from patients with diabetic nephropathy (Figure 3d). To confirm ILK induction in podocytes, we used a double immunostaining for ILK (red) and podocyte marker synaptopodin (green) in diabetic nephropathy. As shown in Figure 3e and f, colocalization of ILK and synaptopodin was evident; and ILK-positive cells were predominantly positioned outside the glomerular basement membrane outlined by synaptopodin in the glomeruli (Figure 3f, arrowheads). These results suggest that ILK is specifically upregulated in the glomerular podocytes of human kidneys with primary glomerular diseases, in which podocyte dysfunction and proteinuria are the major characteristic features.

### Ectopic expression of ILK induces podocyte EMT, migration, and Snail expression

To examine the potential role of ILK induction in podocytes, we investigated the impact of ILK overexpression on podocyte phenotypes and function. Mouse podocytes were infected with adenoviral vector that harbors Flag-tagged ILK gene (Ad.Flag-ILK) or control adenovirus containing  $\beta$ -galactosidase gene (Ad.LacZ), respectively. As shown in Figure 4a, ectopic expression of exogenous ILK suppressed epithelial ZO-1 expression, and induced desmin,  $\alpha$ -smooth muscle actin ( $\alpha$ -SMA) and fibronectin expression in podocytes, as shown by immunofluorescence staining. Flag-tagged ILK expression, as well as desmin,  $\alpha$ -SMA and fibronectin induction after adenoviral vector infection, was confirmed by western blot analysis (Figure 4b). Real-time RT-PCR revealed that ectopic expression of ILK suppressed nephrin expression (Figure 4c). In addition, exogenous ILK also induced MMP-9 expression and secretion, which formed protein aggregates localized on podocyte surface (Figure 4a). These data suggest that forced expression of ILK in podocytes causes a phenotypic change that is reminiscent of EMT.<sup>13</sup>

Podocytes after EMT may become motile with an increased migratory capacity. To test this hypothesis, we examined the effect of ILK on podocyte migration by using a Boyden

chamber motility assay. As shown in Figure 4d and e, ectopic expression of ILK significantly increased the migratory ability of podocytes across the pores of the Transwell filters, suggesting that podocyte EMT induced by ILK is accompanied by an enhanced cell migration.

To explore the potential mechanism underlying ILK regulation of podocyte EMT, we examined the expression of Snail, a key transcription factor that is crucial in controlling EMT in various circumstances. As shown in Figure 4f, ectopic expression of exogenous ILK indeed induced Snail expression in podocytes.

We next examined whether ILK overexpression affects the barrier function of podocyte monolayer. To this end, we used a simple, paracellular albumin flux assay that assesses the albumin filtration across the monolayer of cultured differentiated podocytes. As shown in Figure 4g, an increased albumin flux was observed in the podocytes infected with adenovirus containing ILK gene (Ad.Flag-ILK), when compared with that infected with control adenovirus (Ad.LacZ). These results indicate that ILK overexpression results in a defective filtration barrier and impairs podocyte function.

### **Inhibition of ILK blocks Snail induction and preserves podocyte phenotypes after injury *in vitro***

We next sought to examine whether inhibition of ILK prevents podocyte dysfunction after injury. To test this, we used a highly selective small molecule ILK inhibitor, QLT0267, that has been shown to inhibit ILK signaling in various types of cells.<sup>27–29</sup> The specificity and potency of QLT0267 in inhibiting ILK activity are also shown in kidney tubular epithelial cells.<sup>29</sup> As shown in Figure 5a, QLT0267 selectively inhibited the phosphorylation of glycogen synthase kinase (GSK)-3 $\beta$ , a major downstream substrate of ILK, in podocytes after TGF- $\beta$ 1 stimulation. However, it did not significantly affect the phosphorylation and activation of Smad3 and p38 mitogen-activated protein kinase induced by TGF- $\beta$ 1 (Figure 5a).

Figure 5b shows that QLT0267 effectively blocked Snail expression induced by ILK in podocytes, suggesting that blockade of ILK signaling by QLT0267 is able to inhibit a key EMT initiator gene. Consistently, simultaneous incubation of podocytes with QLT0267 also largely abolished the TGF- $\beta$ 1-mediated induction of desmin, fibronectin, and MMP-9 (Figure 5c–e), thereby preserving podocyte phenotypes.

Inhibition of ILK by QLT0267 also ameliorated podocyte injury induced by ADR, as shown in Figure 6. Mesenchymal transition of podocytes was evident after treatment with ADR, as illustrated by induction of  $\alpha$ -SMA, desmin, fibronectin, and MMP-9 (Figure 6a). These phenotypic alterations were largely prevented by inhibition of ILK with QLT0267 (Figure 6a–c). Hence, ILK could be a therapeutic target for ameliorating ADR-mediated podocyte EMT and dysfunction.

### **Inhibition of ILK ameliorates podocyte injury and prevents albuminuria *in vivo***

We further investigated the role of ILK in podocyte injury and proteinuria *in vivo* by using mouse model of ADR nephropathy. Male BALB/c mice received a single intravenous injection of ADR, and ILK was dramatically upregulated in the isolated glomeruli at 7 days after ADR administration (Figure 7a). Massive albuminuria developed in these mice; and interestingly, daily intraperitoneal administration of QLT0267 significantly ameliorated albuminuria in a dose-dependent manner (Figure 7b). QLT0267 at 5 mg/kg body weight suppressed urine albumin excretion by about 75%, compared with the vehicle controls. Of note, QLT0267 has no adverse effect on normal kidney structure and function.<sup>29</sup>

Figure 8 shows that inhibition of ILK with QLT0267 also ameliorated podocyte injury in ADR nephropathy *in vivo*. Glomeruli were isolated from mouse kidneys after various treatments, and glomerular MMP-9,  $\alpha$ -SMA, and nephrin expression was analyzed by western blot analyses. Consistent with *in vitro* data, ADR-induced MMP-9 and  $\alpha$ -SMA expression in mouse glomeruli, and inhibition of ILK by QLT0267 abrogated their induction (Figure 8a–c). In addition, we found that nephrin expression was suppressed in the glomeruli in ADR nephropathy, compared with normal controls. Consistently, QLT0267 significantly preserved glomerular nephrin expression after ADR injection (Figure 8a and d). Confocal microscopy revealed that whereas nephrin mostly disappeared in ADR-injected mice, it was largely preserved along glomerular basement membrane in the glomeruli after QLT0267 treatment (Figure 8e). Figure 8f shows the quantitative determination of nephrin loss (injury score) in different groups. These data suggest that targeting ILK by small molecule inhibitor is able to ameliorate podocyte injury and prevent proteinuria *in vivo*.

## DISCUSSION

Despite remarkable advances in our understanding of the pathogenesis of proteinuria in patients with genetic, congenital nephrotic syndrome,<sup>4,7</sup> how injurious stimuli cause podocyte damage in many acquired forms of proteinuric kidney diseases such as focal segmental glomerulosclerosis and diabetic nephropathy remains poorly understood. We recently propose that podocytes after injury may undergo a phenotypic conversion that is reminiscent of EMT.<sup>13</sup> Such a phenotypic alteration would certainly cause podocytes to lose their multifaceted morphologic architecture and to relinquish their highly specialized functions, which undoubtedly impairs the integrity of glomerular filtration barrier, leading to the onset of proteinuria. In this study, we have further identified ILK as an important intracellular mediator that controls podocyte EMT. Our results indicate that ILK expression in podocytes is increased in response to various injurious stimuli, and ectopic expression of ILK induces key EMT-regulatory gene *Snail* and promotes podocyte dedifferentiation, migration, and dysfunction. Conversely, specific inhibition of ILK activity by a highly selective small molecule inhibitor ameliorates albuminuria and protects podocytes from injury induced by ADR *in vivo*. These findings provide significant insights into the mechanism underlying podocyte dysfunction in pathologic states, and indicate ILK as a potential therapeutic target for the treatment of proteinuric kidney diseases.

ILK is known to have a central role in regulating a wide variety of cellular processes such as cell adhesion, survival, EMT, and extracellular matrix deposition.<sup>24,30,31</sup> The importance of ILK in podocyte biology is also illustrated clearly in conditional knockout mice in which *ILK* gene is specifically disrupted in podocytes.<sup>19,20</sup> On the other hand, aberrant regulation of ILK occurs in various proteinuric kidney diseases such as nephrotic syndrome, diabetic nephropathy, and experimental models of nephropathies induced by ADR and PAN,<sup>21–23</sup> indicating a close connection between upregulation of ILK and podocyte dysfunction. Notably, ILK expression in podocytes is induced after treatment with a diverse type of injurious stimuli including TGF- $\beta$ 1, ADR, PAN, and high ambient glucose condition (Figures 1 and 2), as well as angiotensin II.<sup>32</sup> ILK is also upregulated in the glomeruli of mouse model of podocyte injury induced by ADR (Figure 7a) and in patients with diabetic nephropathy and focal segmental glomerulosclerosis (Figure 3), two common kidney diseases characterized by prominent proteinuria. As these injurious mediators, including fibrogenic cytokines, toxic, and metabolic factors, are considered as the principal causes of proteinuria, it is conceivable to speculate that increased ILK expression is a common response of podocytes after various injuries, and represents a convergent pathway that mediates podocyte dysfunction and proteinuria under different pathologic conditions. Interestingly,  $\beta$ 1 integrin is also induced in podocytes after incubation with TGF- $\beta$ 1 (Figure 1e) and high glucose.<sup>32</sup> Given that  $\beta$ 1 integrin is a major upstream regulator of ILK, the

simultaneous induction of both  $\beta 1$  integrin and ILK likely leads to an amplification of ILK signaling during podocyte injury.

ILK is well documented as a key intracellular mediator that promotes EMT in different cell systems including tubular epithelial cells.<sup>24,33</sup> As podocytes are capable of undergoing EMT after injury as recently shown,<sup>13,14</sup> the upregulation of ILK in podocytes by a diverse array of injurious stimuli supports the notion that phenotypic alteration could be a potential pathway leading to podocyte dysfunction. Consistent with this view, ectopic expression of exogenous ILK in podocytes not only suppresses nephrin and epithelial ZO-1 expression, but also induces the *de novo* expression of numerous mesenchymal markers including desmin,  $\alpha$ -SMA, fibronectin, and MMP-9 (Figure 4). These alterations in cell-cell adhesion (nephrin and ZO-1) and cytoskeleton (desmin and  $\alpha$ -SMA) proteins will lead to disruption of the slit diaphragm integrity. Interestingly, ectopic expression of ILK renders podocytes to be motile, with an increased migration capacity (Figure 4). This enhanced motility of podocytes after ILK expression could be a part of or a consequence of EMT, which presumably leads to a disruptive glomerular filtration barrier. Indeed, overexpression of ILK impairs the filtration barrier function of podocyte monolayer in a paracellular albumin flux assay (Figure 4). Taken together, our results indicate that upregulation of ILK is sufficient to cause podocyte phenotypic alteration and migration, which is associated with an impaired filtration barrier function.

Although the molecular details by which ILK induces podocyte EMT remain to be elucidated, it seems to be related to its ability to induce Snail expression. ILK is reported to phosphorylate its downstream targets, such as GSK-3 $\beta$ .<sup>34</sup> Phosphorylation of GSK-3 $\beta$  causes its inactivation, which eventually leads to Snail upregulation by different mechanisms. On one hand, inhibition of GSK-3 $\beta$  induces Snail protein stabilization by preventing its phosphorylation and subsequent ubiquitin-mediated degradation;<sup>35</sup> on the other hand, GSK-3 $\beta$  inactivation also stabilizes  $\beta$ -catenin, resulting in its nuclear accumulation, wherein it associates with T-cell factor /lymphoid enhancer-binding factor to regulate Snail gene transcription.<sup>36-38</sup> Consistent with this notion, recent studies show that  $\beta$ -catenin upregulates Snail mRNA expression in mouse podocytes.<sup>26</sup> Hence, ILK-mediated GSK-3 $\beta$  inactivation is able to induce Snail protein expression through both transcriptional and post-translational mechanisms. Accordingly, ectopic expression of ILK markedly induces Snail expression, and inhibition of ILK activity by QLT0267 suppresses Snail induction and blocks TGF- $\beta 1$ - and ADR-induced mesenchymal conversion of podocytes (Figures 5 and 6). Intriguingly, it has been recently shown that Snail directly inhibits nephrin expression in podocytes;<sup>26,39</sup> and fibroblast-specific protein-1-positive podocytes in the urine sediments of patients with diabetic nephropathy selectively express ILK and Snail.<sup>14</sup> In concert, these results point to a critical role of ILK/Snail signaling in mediating podocyte EMT and dysfunction.

This study shows that ILK could be an attractive therapeutic target for the treatment of proteinuric kidney diseases. In mouse model of ADR nephropathy, intraperitoneal injection of QLT0267 suppresses albuminuria in a dose-dependent manner (Figure 7). This beneficial effect of QLT0267 is accompanied by a dose-dependent suppression of MMP-9 and  $\alpha$ -SMA, and a preservation of nephrin expression in the isolated glomeruli of mice after ADR treatment (Figure 8). Therefore, inhibition of ILK activity *in vivo* also blocks the expression of mesenchymal markers ( $\alpha$ -SMA and MMP-9), while prevents loss of podocyte-specific nephrin, consistent with a role of ILK in mediating podocyte phenotypic alteration. The biologic actions of ILK are mediated through its dual functions: as an adapter/scaffolding protein and as a signaling protein.<sup>30,40</sup> As an adapter protein, ILK assumes an important role in normal podocyte biology by bridging the integrin and slit diaphragm signaling through formation of a ternary complex with nephrin.<sup>20</sup> However, it appears that the function of ILK

as an adapter protein in normal physiologic states is independent of its signaling activity, as QLT0267 treatment of normal mice neither disrupts ILK/nephrin interaction nor induces podocyte lesions.<sup>29</sup>

In summary, we have shown in this study that upregulation of ILK is a common response of podocytes after a diverse array of injuries, which may have a role in mediating podocyte EMT, migration, and dysfunction. It should be stressed that this study has some limitations and pitfalls, as it only used an established, transformed podocyte cell line and a single animal model of podocyte injury induced by ADR. Whether these results can extend to primarily cultured podocytes and other proteinuric kidney diseases such as diabetic nephropathy remains to be determined. Nevertheless, our data provide a proof of principle that targeting ILK/Snail pathway with small molecule inhibitor might be an attractive therapeutic strategy for the treatment of proteinuric kidney disorders.

## MATERIALS AND METHODS

### Cell culture and treatment

Mouse conditionally immortalized podocyte cell line was described previously.<sup>41</sup> Cells were cultured on dishes coated with type I collagen (Sigma, St Louis, MO, USA) and in RPMI 1640 medium supplemented with 10% fetal bovine serum, 100 U/ml penicillin, and 100 U/ml streptomycin at 33 °C in the presence of 50 U/ml mouse recombinant  $\gamma$ -interferon (Invitrogen, Carlsbad, CA, USA). To induce differentiation, we grew podocytes under nonpermissive conditions at 37 °C in the absence of interferon- $\gamma$  for 10–14 days, as previously established.<sup>41</sup> Podocytes were treated under differentiating condition in serum-free medium with TGF- $\beta$ 1 (R&D Systems, Minneapolis, MN, USA), ADR (doxorubicin hydrochloride; Sigma), PAN, and high glucose (Sigma) at different concentrations for various periods of time as indicated. For high-glucose treatment, glucose was added to the glucose-free medium to final concentrations of 5 mM (normal glucose) or 30 mM (high glucose), respectively. Mannitol was used as controls (5 mM glucose + 25 mM mannitol). Podocytes were refed with fresh medium containing high glucose or mannitol every 3 days.

### Animal studies

Male BALB/c mice weighing 20–22 g were obtained from Harlan Sprague Dawley (Indianapolis, IN, USA) and housed in the animal facilities of the University of Pittsburgh Medical Center, with free access to food and water. Animals were treated humanely by use of the protocols approved by the institutional animal use and care committee at the University of Pittsburgh. Mice were injected through the tail vein with ADR at the dosage of 12 mg/kg body weight in saline solution. Small molecule ILK inhibitor QLT0267 (generously provided by QLT, Vancouver, BC, Canada) was administered by daily intraperitoneal injection at the doses of 0.5, 2.0, and 5.0 mg/kg body weight. As a control, a group of ADR mice was injected with the same volume of vehicle (5% Tween 80 in 0.9% saline). Animals were killed at day 7 after ADR injection. The kidneys were removed for various analyses. One part of the kidney was fixed in 10% phosphate-buffered formalin, followed by paraffin embedding for histologic and immunohistochemical studies. Another part of kidneys was used to isolate renal glomeruli by a sequential sieving technique as described previously.<sup>42</sup> The third part was snap-frozen in liquid nitrogen, and stored at –80 °C for cryosections and protein extractions.

### Adenovirus infection

Podocytes were seeded in complete medium on six-well plates, and infected with adenovirus that harbors Flag-tagged ILK gene (Ad.Flag-ILK),<sup>43</sup> or the control adenovirus containing  $\beta$ -galactosidase gene (Ad.LacZ) at a concentration of 2 or 4  $\times 10^7$  particles per ml. Infected

cells were incubated for 6 h, and then restored to complete medium. After 48 h, whole-cell lysates were collected for real-time RT-PCR and western blot analyses. Infected cells were also subjected to immunofluorescence staining with different antibodies, respectively.

### Western blot analysis

Proteins in cell and glomerular lysates were separated on SDS–polyacrylamide gel electrophoresis and detected by western blot analysis according to the established protocols described previously.<sup>44</sup> The primary antibodies used were as follows: anti-ILK (Upstate, Charlottesville, VA, USA), anti- $\beta$ 1 integrin (cat. no. 610468), anti-fibronectin (clone 10) (BD Transduction Laboratories, Lexington, KY, USA), anti-MMP-9, anti- $\alpha$ -SMA (clone 1A4), anti- $\alpha$ -tubulin (T-9026) (Sigma), anti-desmin (MP Biomedicals, Solon, OH, USA), anti-Snail (Ab17732; Abcam, Cambridge, MA, USA), anti-phosphorylated GSK-3 $\beta$  (cat. no. 9336), total GSK-3 $\beta$  (cat. no. 9315), anti-phosphorylated Smad3 (cat. no. 9514), anti-phosphorylated p38 mitogen-activated protein kinase (cat. no. 4631) (Cell Signaling Technology, Danvers, MA, USA), anti-nephrin (Fitzgerald Industries International, Concord, MA, USA), anti-Smad1/2/3 (sc-7960), anti-actin (sc-1616) (Santa Cruz Biotechnology, Santa Cruz, CA), anti-glyceraldehyde 3-phosphate dehydrogenase (Ambion, Austin, TX, USA).

### Immunofluorescence staining

Podocytes grown on type I collagen-coated cover-slips and kidney cryosections at 4- $\mu$ m thickness were fixed for 15 min at room temperature in 4% paraformaldehyde, followed by permeabilization with 0.2% Triton X-100 in phosphate-buffered saline for 10 min. After blocking with 10% normal donkey serum in phosphate-buffered saline for 30 min, cells and kidney sections were incubated with primary antibodies against ILK, fibronectin,  $\alpha$ -SMA, desmin, MMP-9, ZO-1, nephrin, and podocalyxin (Zymed, Carlsbad, CA, USA). Nonimmune immunoglobulin G served as a negative control, and no staining was observed. The slides were viewed under Eclipse E600 epifluorescence microscope, or Leica TCS-SL confocal microscope. A semiquantitative scoring was performed to determine the severity of injury. Score 0 represents no lesion, 1, 2, 3, and 4 represent the lesion involving <25, 25–50, 50–75, and >75% of the glomerular tuft area, respectively. At least 10 glomeruli were randomly selected for each mouse and then an average of composite score was calculated. Three mice from each group were analyzed.

### Immunostaining for human kidney specimens

Human kidney specimens were obtained from diagnostic renal biopsy performed at the University of Pittsburgh Medical Center. As normal controls, nontumor kidney tissue from the patients who had renal cell carcinoma and underwent nephrectomy was used. Studies using human tissues were approved by the institutional review board at the University of Pittsburgh. Immunohistochemical staining was performed using established procedures as described previously.<sup>13,45</sup> Briefly, paraffin-embedded kidney sections from patients were prepared by a routine procedure and stained with the specific primary antibody against ILK (Upstate). As a negative control, the primary antibody was replaced with nonimmune goat immunoglobulin G, and no staining occurred. To confirm ILK expression in podocytes, we performed double immunofluorescence staining for ILK and podocyte marker synaptopodin on human kidney specimens. Briefly, paraffin-embedded kidney sections were incubated with primary antibodies against ILK and synaptopodin (Progen, Heidelberg, Germany), followed by staining with FITC- and CY3-conjugated secondary antibodies. Stained samples were viewed using an Eclipse E600 epifluorescence microscope equipped with a digital camera (Nikon, Melville, NY, USA).



### Real-time RT-PCR

For quantitative determination of nephrin mRNA levels, a real-time RT-PCR was performed on ABI PRISM 7000 Sequence Detection System (Applied Biosystems, Foster City, CA, USA), as described previously.<sup>29</sup> Total RNA was extracted using TRIzol RNA isolation system (Invitrogen). The first strand of cDNA was synthesized using 2 µg RNA in 20 µl of reaction buffer by RT using AMV-RT (Promega, Madison, WI, USA) and random primers at 42 °C for 30 min. The PCR reaction mixture in a 25 µl volume contained 12.5 µl 2 × SYBR Green PCR Master Mix (Applied Biosystems), 5 µl diluted RT product (1:10), and 0.5 µM sense and antisense primer sets. The sequences of β-actin primer pairs used in real-time PCR were described previously.<sup>29</sup> The sequences of nephrin primer pairs were as follows: 5'-cccaggtacacagagcaca (sense), and 5'-ctcacgctca caaccttcag (antisense). PCR reaction was run under standard conditions. After sequential incubations at 50 °C for 2 min and 95 °C for 10 min, respectively, the amplification protocol consisted of 50 cycles of denaturing at 95 °C for 15 s, annealing and extension at 60 °C for 60 s. The standard curve was constructed from series dilutions of template cDNA. The nephrin mRNA levels were calculated after normalizing with β-actin.

### Boyden chamber motility assay

Cell motility and migration were evaluated using Boyden chamber motogenicity assay with tissue culture-treated Transwell filters (Corning Costar Corporation, Cambridge, MA, USA), as described previously.<sup>46</sup> Podocytes after infection with Ad.Flag-ILK or Ad.LacZ adenovirus were seeded onto the filters (8 µm pore size) in the top compartment of the chamber. After 2 days of incubation at 37 °C filters were fixed with 3% paraformaldehyde in phosphate-buffered saline, and stained with 0.1% Coomassie blue in 10% methanol–10% acetic acid, and the upper surface of the filters was carefully wiped with a cotton-tipped applicator. Cells that passed through the pores were counted in three nonoverlapping × 20 fields and photographed with a Nikon microscope.

### Albumin influx assay

Albumin filtration assay was performed by measuring the transepithelial passage of bovine serum albumin from bottom to top compartment of the Transwell chambers (0.4 µm pore; Corning Costar Corporation) as described previously.<sup>47–49</sup> Confluent differentiated podocytes were exposed to adenovirus containing ILK gene (Ad.Flag-ILK) or control adenovirus (Ad.LacZ) for 48 h. Cells were washed twice with phosphate-buffered saline supplemented with 1 mM MgCl<sub>2</sub> and 1 mM CaCl<sub>2</sub> to preserve the cadherin-based junctions. The top chamber was then refilled with 0.15 ml RPMI 1640 and the bottom chamber with 1 ml RPMI 1640 supplemented with 40 mg/ml bovine serum albumin and incubated for 1 h at 37 °C. At the end of the incubation, albumin concentration in the top chamber was determined using a bicinchoninic acid protein assay kit (Sigma) with bovine serum albumin as a standard.

### Urine albumin and creatinine assay

Urine albumin was determined by using a mouse albumin enzyme linked immunosorbent assay Quantitation kit, according to the manufacturer's protocol (Bethyl Laboratories, Montgomery, TX, USA).<sup>20</sup> Urine creatinine was measured by using Quantichrome creatinine assay kit, according to the protocol specified by the manufacturer (BioAssay Systems, Hayward, CA, USA).

### Statistical analyses

All data examined were expressed as mean ± s.e.m. Statistical analysis of the data was performed by using SigmaStat software (Jandel Scientific, San Rafael, CA, USA).

Comparison between groups was carried out using one-way analysis of variance, followed by Student–Newman–Keuls test.  $P < 0.05$  was considered statistically significant.

## Acknowledgments

This work was supported by the National Institutes of Health Grants DK061408, DK064005 and DK071040 (YL), and DK054639 (CW).

## REFERENCES

1. Shankland SJ. The podocyte's response to injury: role in proteinuria and glomerulosclerosis. *Kidney Int.* 2006; 69:2131–2147. [PubMed: 16688120]
2. Wiggins RC. The spectrum of podocytopathies: a unifying view of glomerular diseases. *Kidney Int.* 2007; 71:1205–1214. [PubMed: 17410103]
3. Pavenstadt H, Kriz W, Kretzler M. Cell biology of the glomerular podocyte. *Physiol Rev.* 2003; 83:253–307. [PubMed: 12506131]
4. Tryggvason K, Wartiovaara J. Molecular basis of glomerular permselectivity. *Curr Opin Nephrol Hypertens.* 2001; 10:543–549. [PubMed: 11458036]
5. Reiser J, Kriz W, Kretzler M, et al. The glomerular slit diaphragm is a modified adherens junction. *J Am Soc Nephrol.* 2000; 11:1–8. [PubMed: 10616834]
6. Kerjaschki D. Caught flat-footed: podocyte damage and the molecular bases of focal glomerulosclerosis. *J Clin Invest.* 2001; 108:1583–1587. [PubMed: 11733553]
7. Durvasula RV, Shankland SJ. Podocyte injury and targeting therapy: an update. *Curr Opin Nephrol Hypertens.* 2006; 15:1–7. [PubMed: 16340659]
8. Kanjanabuch T, Ma LJ, Chen J, et al. PPAR-gamma agonist protects podocytes from injury. *Kidney Int.* 2007; 71:1232–1239. [PubMed: 17457378]
9. Susztak K, Raff AC, Schiffer M, et al. Glucose-induced reactive oxygen species cause apoptosis of podocytes and podocyte depletion at the onset of diabetic nephropathy. *Diabetes.* 2006; 55:225–233. [PubMed: 16380497]
10. Wharram BL, Goyal M, Wiggins JE, et al. Podocyte depletion causes glomerulosclerosis: diphtheria toxin-induced podocyte depletion in rats expressing human diphtheria toxin receptor transgene. *J Am Soc Nephrol.* 2005; 16:2941–2952. [PubMed: 16107576]
11. Mitu GM, Wang S, Hirschberg R. BMP7 is a podocyte survival factor and rescues podocytes from diabetic injury. *Am J Physiol Renal Physiol.* 2007; 293:F1641–F1648. [PubMed: 17804487]
12. Yu D, Petermann A, Kunter U, et al. Urinary podocyte loss is a more specific marker of ongoing glomerular damage than proteinuria. *J Am Soc Nephrol.* 2005; 16:1733–1741. [PubMed: 15829708]
13. Li Y, Kang YS, Dai C, et al. Epithelial-to-mesenchymal transition is a potential pathway leading to podocyte dysfunction and proteinuria. *Am J Pathol.* 2008; 172:299–308. [PubMed: 18202193]
14. Yamaguchi Y, Iwano M, Toyoda M, et al. Epithelial–mesenchymal transition as an explanation for podocyte depletion in diabetic nephropathy. *Am J Kidney Dis.* 2009; 54:653–664. [PubMed: 19615802]
15. Reidy K, Susztak K. Epithelial–mesenchymal transition and podocyte loss in diabetic kidney disease. *Am J Kidney Dis.* 2009; 54:590–593. [PubMed: 19781451]
16. Liu Y. New insights into epithelial–mesenchymal transition in kidney fibrosis. *J Am Soc Nephrol.* 2010; 21:212–222. [PubMed: 20019167]
17. Yoganathan N, Yee A, Zhang Z, et al. Integrin-linked kinase, a promising cancer therapeutic target: biochemical and biological properties. *Pharmacol Ther.* 2002; 93:233–242. [PubMed: 12191615]
18. Hannigan G, Troussard AA, Dedhar S. Integrin-linked kinase: a cancer therapeutic target unique among its ILK. *Nat Rev Cancer.* 2005; 5:51–63. [PubMed: 15630415]
19. El-Aouni C, Herbach N, Blattner SM, et al. Podocyte-specific deletion of integrin-linked kinase results in severe glomerular basement membrane alterations and progressive glomerulosclerosis. *J Am Soc Nephrol.* 2006; 17:1334–1344. [PubMed: 16611717]

20. Dai C, Stolz DB, Bastacky SI, et al. Essential role of integrin-linked kinase in podocyte biology: bridging the integrin and slit diaphragm signaling. *J Am Soc Nephrol.* 2006; 17:2164–2175. [PubMed: 16837631]
21. Teixeira Vde P, Blattner SM, Li M, et al. Functional consequences of integrin-linked kinase activation in podocyte damage. *Kidney Int.* 2005; 67:514–523. [PubMed: 15673299]
22. Kretzler M, Teixeira VP, Unschuld PG, et al. Integrin-linked kinase as a candidate downstream effector in proteinuria. *FASEB J.* 2001; 15:1843–1845. [PubMed: 11481249]
23. Guo L, Sanders PW, Woods A, et al. The distribution and regulation of integrin-linked kinase in normal and diabetic kidneys. *Am J Pathol.* 2001; 159:1735–1742. [PubMed: 11696434]
24. Li Y, Yang J, Dai C, et al. Role for integrin-linked kinase in mediating tubular epithelial to mesenchymal transition and renal interstitial fibrogenesis. *J Clin Invest.* 2003; 112:503–516. [PubMed: 12925691]
25. Wang Y, Wang YP, Tay YC, et al. Progressive adriamycin nephropathy in mice: sequence of histologic and immunohistochemical events. *Kidney Int.* 2000; 58:1797–1804. [PubMed: 11012915]
26. Dai C, Stolz DB, Kiss LP, et al. Wnt/ $\beta$ -catenin signaling promotes podocyte dysfunction and albuminuria. *J Am Soc Nephrol.* 2009; 20:1997–2008. [PubMed: 19628668]
27. Oloumi A, Syam S, Dedhar S. Modulation of Wnt3a-mediated nuclear beta-catenin accumulation and activation by integrin-linked kinase in mammalian cells. *Oncogene.* 2006; 25:7747–7757. [PubMed: 16799642]
28. Koul D, Shen R, Bergh S, et al. Targeting integrin-linked kinase inhibits Akt signaling pathways and decreases tumor progression of human glioblastoma. *Mol Cancer Ther.* 2005; 4:1681–1688. [PubMed: 16275989]
29. Li Y, Tan X, Dai C, et al. Inhibition of integrin-linked kinase attenuates renal interstitial fibrosis. *J Am Soc Nephrol.* 2009; 20:1907–1918. [PubMed: 19541809]
30. Legate KR, Montanez E, Kudlacek O, et al. ILK, PINCH and parvin: the tIPP of integrin signalling. *Nat Rev Mol Cell Biol.* 2006; 7:20–31. [PubMed: 16493410]
31. Wu C. PINCH, N(i)ck and the ILK: network wiring at cell–matrix adhesions. *Trends Cell Biol.* 2005; 15:460–466. [PubMed: 16084094]
32. Han SY, Kang YS, Jee YH, et al. High glucose and angiotensin II increase beta1 integrin and integrin-linked kinase synthesis in cultured mouse podocytes. *Cell Tissue Res.* 2006; 323:321–332. [PubMed: 16189717]
33. Wu C, Keightley SY, Leung-Hagesteijn C, et al. Integrin-linked protein kinase regulates fibronectin matrix assembly, E-cadherin expression, and tumorigenicity. *J Biol Chem.* 1998; 273:528–536. [PubMed: 9417112]
34. Delcommenne M, Tan C, Gray V, et al. Phosphoinositide-3-OH kinase-dependent regulation of glycogen synthase kinase 3 and protein kinase B/AKT by the integrin-linked kinase. *Proc Natl Acad Sci USA.* 1998; 95:11211–11216. [PubMed: 9736715]
35. Zhou BP, Deng J, Xia W, et al. Dual regulation of Snail by GSK-3beta-mediated phosphorylation in control of epithelial–mesenchymal transition. *Nat Cell Biol.* 2004; 6:931–940. [PubMed: 15448698]
36. Troussard AA, Costello P, Yoganathan TN, et al. The integrin linked kinase (ILK) induces an invasive phenotype via AP-1 transcription factor-dependent upregulation of matrix metalloproteinase 9 (MMP-9). *Oncogene.* 2000; 19:5444–5452. [PubMed: 11114721]
37. D’Amico M, Hulit J, Amanatullah DF, et al. The integrin-linked kinase regulates the cyclin D1 gene through glycogen synthase kinase 3beta and cAMP-responsive element-binding protein-dependent pathways. *J Biol Chem.* 2000; 275:32649–32657. [PubMed: 10915780]
38. Tan C, Costello P, Sanghera J, et al. Inhibition of integrin linked kinase (ILK) suppresses beta-catenin-Lef/Tcf-dependent transcription and expression of the E-cadherin repressor, snail, in APC  $-/-$  human colon carcinoma cells. *Oncogene.* 2001; 20:133–140. [PubMed: 11244511]
39. Matsui I, Ito T, Kurihara H, et al. Snail, a transcriptional regulator, represses nephrin expression in glomerular epithelial cells of nephrotic rats. *Lab Invest.* 2007; 87:273–283. [PubMed: 17260001]

40. Li Y, Dai C, Wu C, et al. PINCH-1 promotes tubular epithelial-to-mesenchymal transition by interacting with integrin-linked kinase. *J Am Soc Nephrol.* 2007; 18:2534–2543. [PubMed: 17656471]
41. Mundel P, Reiser J, Zuniga Mejia Borja A, et al. Rearrangements of the cytoskeleton and cell contacts induce process formation during differentiation of conditionally immortalized mouse podocyte cell lines. *Exp Cell Res.* 1997; 236:248–258. [PubMed: 9344605]
42. Liu Y, Tolbert EM, Sun AM, et al. Primary structure of rat HGF receptor and induced expression in glomerular mesangial cells. *Am J Physiol.* 1996; 271:F679–F688. [PubMed: 8853431]
43. Guo L, Wu C. Regulation of fibronectin matrix deposition and cell proliferation by the PINCH-ILK-CH-ILKBP complex. *FASEB J.* 2002; 16:1298–1300. [PubMed: 12060675]
44. Yang J, Shultz RW, Mars WM, et al. Disruption of tissue-type plasminogen activator gene in mice reduces renal interstitial fibrosis in obstructive nephropathy. *J Clin Invest.* 2002; 110:1525–1538. [PubMed: 12438450]
45. Tan X, Wen X, Liu Y. Paricalcitol inhibits renal inflammation by promoting vitamin D receptor-mediated sequestration of NF- $\kappa$ B signaling. *J Am Soc Nephrol.* 2008; 19:1741–1752. [PubMed: 18525004]
46. Yang J, Liu Y. Dissection of key events in tubular epithelial to myofibroblast transition and its implications in renal interstitial fibrosis. *Am J Pathol.* 2001; 159:1465–1475. [PubMed: 11583974]
47. Li X, Yuan H, Zhang X. Adriamycin increases podocyte permeability: evidence and molecular mechanism. *Chin Med J.* 2003; 116:1831–1835. [PubMed: 14687468]
48. Hunt JL, Pollak MR, Denker BM. Cultured podocytes establish a size-selective barrier regulated by specific signaling pathways and demonstrate synchronized barrier assembly in a calcium switch model of junction formation. *J Am Soc Nephrol.* 2005; 16:1593–1602. [PubMed: 15843471]
49. Rico M, Mukherjee A, Konieczkowski M, et al. WT1-interacting protein and ZO-1 translocate into podocyte nuclei after puromycin aminonucleoside treatment. *Am J Physiol Renal Physiol.* 2005; 289:F431–F441. [PubMed: 15798086]

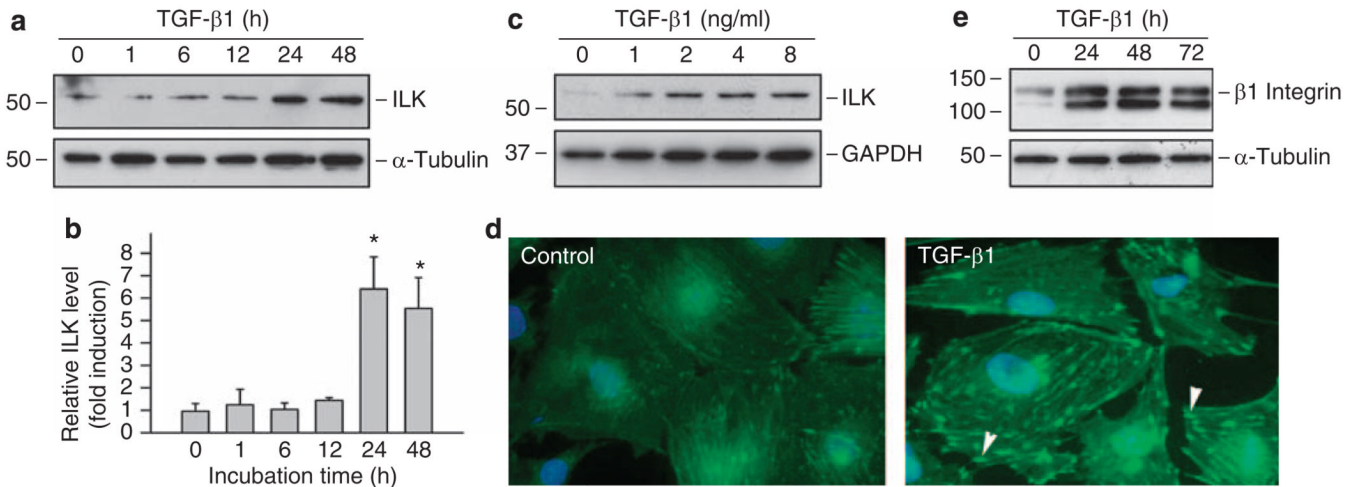


**Figure 1. TGF-β1 induces ILK and β1 integrin expression in mouse podocytes**

(a–c) Western blot analyses show that TGF-β1 induced ILK expression in cultured podocytes in a time- and dose-dependent manner. Podocytes were incubated with 2 ng/ml of TGF-β1 for various periods of time as indicated (a, b) or with different concentrations of TGF-β1 for 48 h (c). Quantitative determination of relative ILK levels in different times after TGF-β1 treatment was presented in (b). \* $P < 0.05$  versus controls ( $n = 3$ ). (d) Immunofluorescence staining showed ILK induction by TGF-β1 in podocytes. ILK protein was specifically localized at the focal adhesion sites of podocytes (arrowheads). (e) TGF-β1 (2 ng/ml) also induced β1 integrin expression in mouse podocytes. GAPDH, glyceraldehyde 3-phosphate dehydrogenase; ILK, integrin-linked kinase; TGF-β1, transforming growth factor-β1.

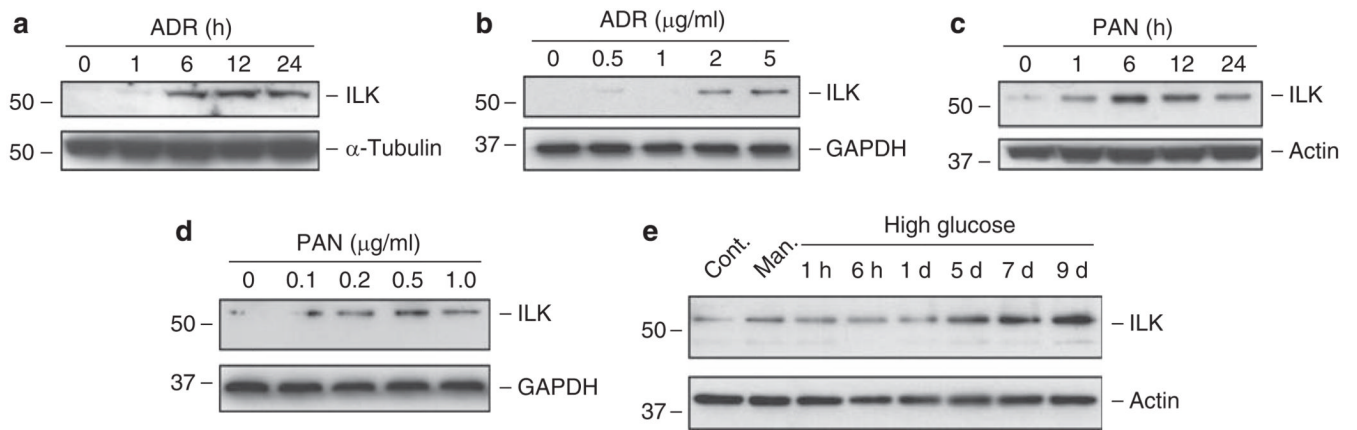


**Figure 2. Induction of ILK expression in podocytes in response to various injurious stimuli**

Podocytes were treated with 2  $\mu$ g/ml of adriamycin (a) or with 1  $\mu$ g/ml of puromycin aminonucleoside (c) for various periods of time as indicated, or with increasing amounts of ADR (b) and PAN (d) for 12 h. Podocytes were also incubated with high glucose (30 mM) for different periods of time as indicated (e). Both normal glucose (5 mM) and mannitol (5 mM normal glucose and 25 mM mannitol) were used as controls and harvested at 9 days. Cell lysates were immunoblotted with antibodies against ILK and housekeeping proteins. ADR, adriamycin; Cont. Man., control mannitol; GAPDH, glyceraldehyde 3-phosphate dehydrogenase; ILK, integrin-linked kinase; PAN, puromycin aminonucleoside.

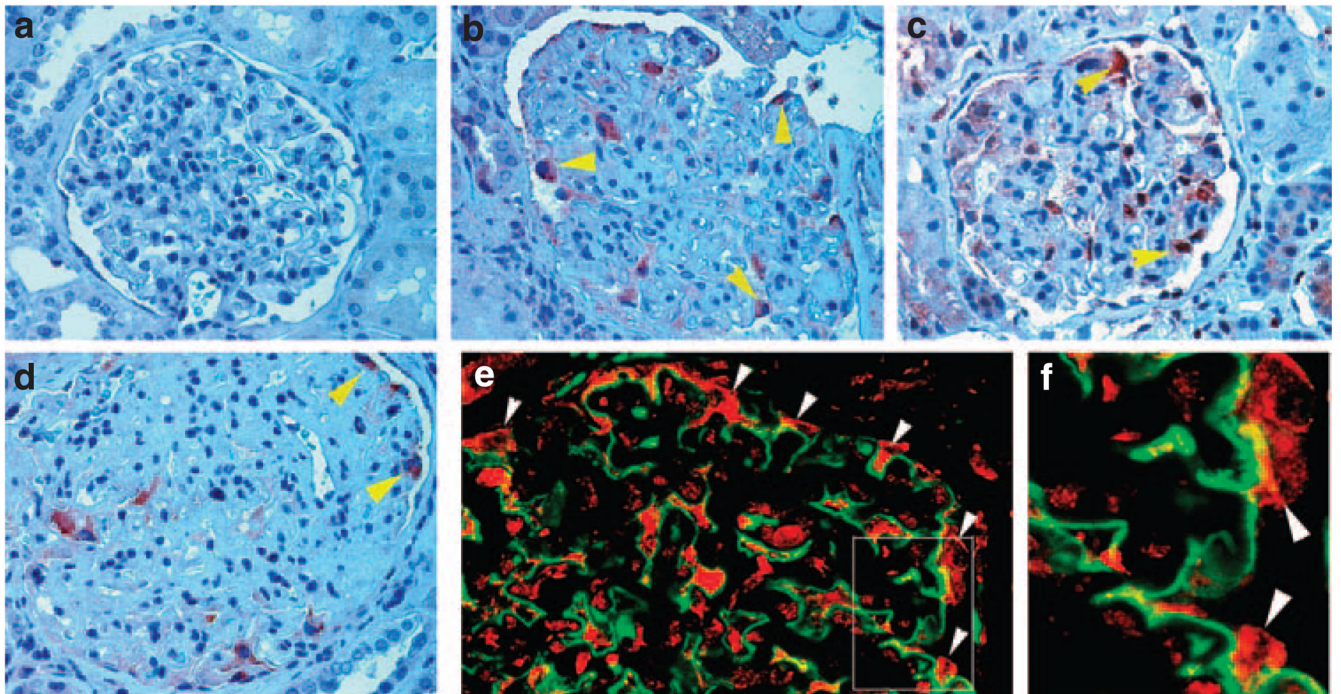


**Figure 3. Induction of ILK protein in the glomerular podocytes in patients with proteinuric kidney diseases**

Immunohistochemical staining showed strong ILK expression in the glomerular podocytes of patients with proteinuric kidney diseases. (a) normal kidney; (b) focal segmental glomerulosclerosis; (c) focal segmental glomerulosclerosis; (d) diabetic nephropathy. (e) Double immunofluorescence staining shows ILK localization in glomerular podocytes. Kidney biopsies from patients with diabetic nephropathy were double immunostained for ILK (red) and podocyte marker synaptopodin (green). (f) Enlarged box area in (e). Arrowheads indicate positive staining.

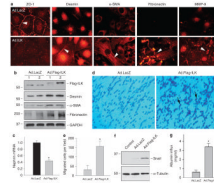


**Figure 4. Ectopic expression of ILK induces podocyte EMT, migration, and Snail expression**

**(a)** Immunofluorescence staining showed that exogenous ILK expression resulted in suppression of ZO-1 and induction of mesenchymal marker desmin,  $\alpha$ -SMA, fibronectin, and MMP-9 in podocytes. Podocytes were infected with adenovirus harboring either Flag-ILK (Ad.Flag-ILK) or  $\beta$ -galactosidase gene (Ad.LacZ). Overexpression of exogenous ILK (Flag-ILK) and induction of desmin,  $\alpha$ -SMA and fibronectin in podocytes were also confirmed by western blot analysis **(b)**. Of note, infection with control adenovirus (Ad.LacZ) did not significantly affect the basal expression of ILK, desmin,  $\alpha$ -SMA and fibronectin. **(c)** Real-time RT-PCR showed that ectopic expression of exogenous ILK inhibited nephrin mRNA expression. Relative mRNA level over the Ad.LacZ controls (value = 1.0) is presented.  $*P < 0.05$  ( $n = 6$ ). **(d, e)** Forced expression of ILK promoted podocyte migration. Representative micrographs show podocyte migration in a Boyden chamber motility assay **(d)**. Quantitative determination of the migrated podocytes per field in different groups is presented **(e)**.  $*P < 0.05$  ( $n = 3$ ). **(f)** Ectopic expression of ILK induced Snail expression. Cell lysates were prepared at 48 h after infection with Ad.Flag-ILK or Ad.LacZ adenovirus, and immunoblotted with antibodies against Snail and  $\alpha$ -tubulin, respectively. Cells without infection with adenovirus were denoted as control. **(g)** Overexpression of ILK impaired the filtration barrier function of podocytes. Podocyte monolayer on collagen-coated Transwell filters was infected with Ad.LacZ or Ad.Flag-ILK adenovirus, and 24 h later albumin permeability across podocyte monolayer was determined. Data are presented as means  $\pm$  s.e.m. ( $n = 6$ ).  $*P < 0.01$  versus Ad.LacZ control.  $\alpha$ -SMA,  $\alpha$ -smooth muscle actin; EMT, epithelial–mesenchymal transition, GAPDH, glyceraldehyde 3-phosphate dehydrogenase; ILK, integrin-linked kinase; MMP-9, matrix metalloproteinase-9.



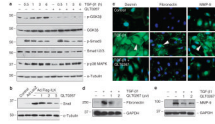


**Figure 5. Targeting ILK activity by small molecule inhibitor QLT0267 abolishes Snail induction and blocks mesenchymal conversion of podocytes**

(a) Small molecule ILK inhibitor QLT0267 selectively inhibited the TGF- $\beta$ 1-induced phosphorylation of GSK-3 $\beta$ , but not Smad3 and p38 MAPK. Podocytes were pretreated with QLT0267 (10  $\mu$ M) for 0.5 h, followed by incubation with TGF- $\beta$ 1 (2 ng/ml) for different periods of time as indicated. Cell lysates were immunoblotted with various antibodies as indicated. (b) QLT0267 blocked ILK-induced Snail expression in podocytes. Podocytes were infected with Ad.Flag-ILK or Ad.LacZ adenovirus. At 24 h later, cells were treated with different doses of QLT0267 as indicated for additional 24 h. Cell lysates were immunoblotted with specific antibodies against Snail and  $\alpha$ -tubulin. (c) Immunofluorescence staining showed that QLT0267 inhibited the desmin, fibronectin, and MMP-9 expression induced by TGF- $\beta$ 1 in podocytes. (d, e) Western blot analyses showed that QLT0267 inhibited the TGF- $\beta$ 1-mediated fibronectin and MMP-9 expression in a dose-dependent manner. Podocytes were treated without or with TGF- $\beta$ 1 (2 ng/ml) in the absence or presence of different doses of QLT0267 as indicated. GAPDH, glyceraldehyde 3-phosphate dehydrogenase; GSK-3 $\beta$ , glycogen synthase kinase-3 $\beta$ ; ILK, integrin-linked kinase; MAPK, mitogen-activated protein kinase; MMP-9, matrix metalloproteinase-9; TGF- $\beta$ 1, transforming growth factor- $\beta$ 1.

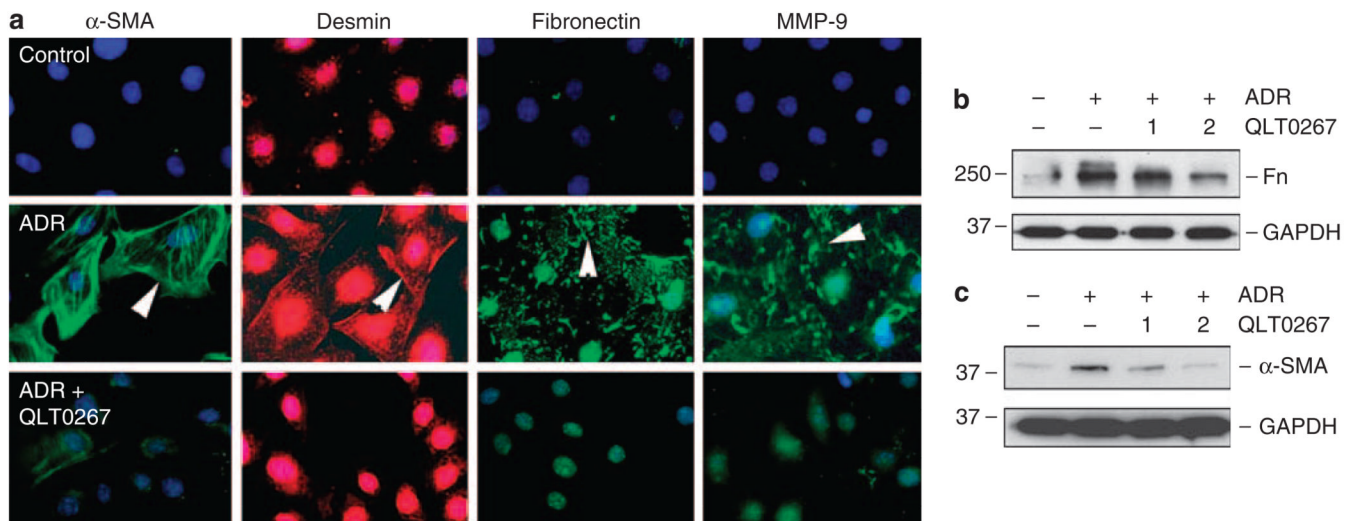


**Figure 6. QLT0267 also blocks the ADR-mediated mesenchymal conversion of podocytes**  
**(a)** Immunofluorescence staining showed that QLT0267 inhibited the  $\alpha$ -SMA, desmin, fibronectin, and MMP-9 expression induced by ADR in podocytes. **(b, c)** Western blot analyses showed that QLT0267 dose dependently inhibited the ADR-mediated fibronectin and  $\alpha$ -SMA expression in podocytes. Doses of QLT0267 (1 and 2  $\mu\text{M}$ ) are indicated. ADR, adriamycin;  $\alpha$ -SMA,  $\alpha$ -smooth muscle actin; Fn, fibronectin; GAPDH, glyceraldehyde 3-phosphate dehydrogenase.

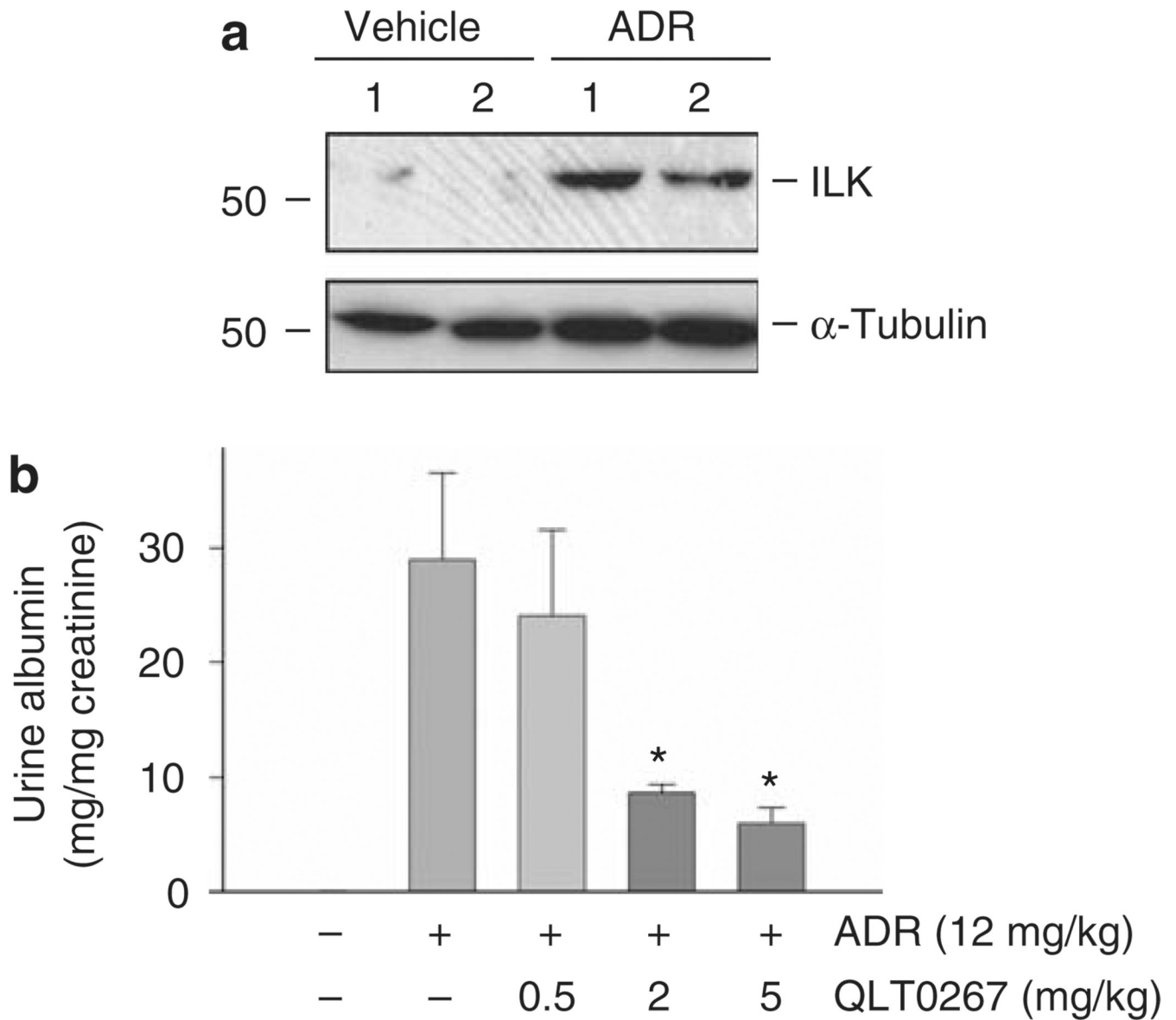


**Figure 7. Targeting ILK *in vivo* ameliorates albuminuria after ADR injury**

(a) Upregulation of ILK in the glomeruli *in vivo* after podocyte injury induced by ADR.

Glomeruli were isolated from mice injected with ADR for 7 days. Whole-glomerular lysates were immunoblotted with antibodies against ILK and  $\alpha$ -tubulin. Numbers (1 and 2) indicate each individual animal in a given group. (b) Inhibition of ILK activity by QLT0267 reduced albuminuria in ADR nephropathy. Mice injected with ADR were administered with different doses of QLT0267 for 7 days. Urinary albumin level was determined and corrected to urine creatinine. Urine albumin was expressed as mg per mg creatinine and presented as mean  $\pm$  s.e.m. \* $P < 0.05$  versus ADR alone ( $n = 6$ ). ADR, adriamycin; ILK, integrin-linked kinase.

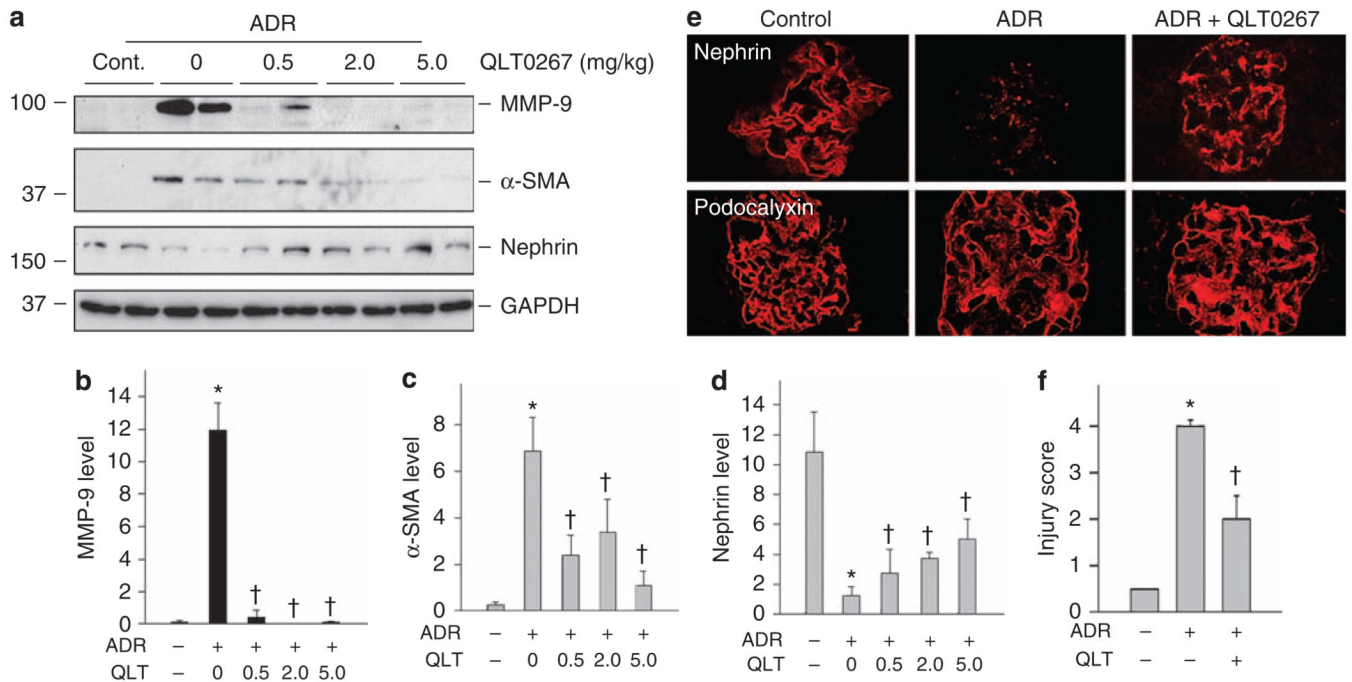


**Figure 8. Targeting ILK *in vivo* ameliorates the ADR-mediated glomerular injury and preserves nephrin expression**

(a–d) Whole-glomerular lysates were analyzed by western blotting using specific antibodies against MMP-9,  $\alpha$ -SMA, nephrin, and GAPDH. (a) Representative western blots. (b–d) Quantitative data on MMP-9 (b),  $\alpha$ -SMA (c), and nephrin (d) are presented as mean  $\pm$  s.e.m. ( $n = 6$ ). \* $P < 0.05$  versus normal controls, † $P < 0.05$  versus ADR alone controls. (e) Confocal immunofluorescence microscopy showed the distribution of nephrin and podocalyxin in mouse glomeruli at 7 days after ADR injection. QLT0267 largely preserved nephrin expression after ADR. (f) Semiquantitative evaluation on nephrin loss (injury score) in the glomeruli among different groups. \* $P < 0.05$  versus normal controls, † $P < 0.05$  versus ADR alone ( $n = 6$ ). ADR, adriamycin;  $\alpha$ -SMA,  $\alpha$ -smooth muscle actin; GAPDH, glyceraldehyde 3-phosphate dehydrogenase; ILK, integrin-linked kinase; MMP-9, matrix metalloproteinase-9.